

We wish to thank Dr. Sidney Putnam for pointing out the relevancy of the pressure balance viewpoint in interpreting our findings and Dr. Gerold Yonas for helpful conversations.

\*This work was supported by DNA Contract 71-C-0052.

<sup>1</sup>G. Yonas, I. Smith, P. Spence, S. Putnam, and P. Champney, in Proceedings of the Eleventh Symposium on Electron, Ion, and Laser Beam Technology, Boulder, Colorado, May 1971 (to be published); J. Block, J. Burton, J. Frame, D. Hammer, A. Kolb, L. Levine, W. Lupton, W. Oliphant, J. Shipman, and I. Vitkovitsky, *ibid.*

<sup>2</sup>G. Yonas, P. Spence, D. Pellinent, B. Ecker, and S. Heurlin, Physics International Company Report No. PIFR-106-1, 1969 (unpublished).

<sup>3</sup>W. L. Gardner and J. A. Nation, *Bull. Amer. Phys. Soc.* **16**, 1251 (1971).

<sup>4</sup>L. P. Bradley, Sandia Laboratories, private communication.

<sup>5</sup>T. G. Roberts and W. H. Bennett, *Plasma Phys.* **10**, 381 (1968).

<sup>6</sup>J. Benford and B. Ecker, *Phys. Rev. Lett.* **26**, 1160 (1971).

<sup>7</sup>B. Ecker, J. Benford, C. Stallings, P. Spence, and S. Putnam, in Proceedings of the Eleventh Symposium on Electron, Ion, and Laser Beam Technology, Boulder, Colorado, May 1971 (to be published).

<sup>8</sup>G. Yonas and P. Spence, in *Record of the Tenth Symposium on Electron, Ion, and Laser Beam Technology*, edited by L. Marton (San Francisco Press, San Francisco, Calif., 1969).

<sup>9</sup>A. A. Ivanov and L. I. Rudakov, *Zh. Eksp. Teor. Fiz.* **58**, 1332 (1970) [*Sov. Phys. JETP* **31**, 715 (1970)].

<sup>10</sup>R. Lee and R. N. Sudan, *Phys. Fluids* **14**, 1213 (1971).

<sup>11</sup>In this density regime ( $\sim 10^{16}$  cm<sup>-3</sup>) there is no evidence of the usual beam-plasma instabilities. Collisions in the background plasma and the large parallel energy spread of the beam may be responsible.

<sup>12</sup>S. Putnam, Physics International Company Report No. PIFR-105, 1971 (unpublished).

## Nonstationary Behavior of Collisionless Shocks\*

D. L. Morse, W. W. Destler, and P. L. Auer

*Laboratory of Plasma Studies, Cornell University, Ithaca, New York 14850*

(Received 1 November 1971)

Laboratory measurements indicate that a collisionless shock wave formed in a plasma-wind-tunnel device is nonstationary on the time scale of the ion gyroperiod. This behavior suggests a possible interpretation of recent data on magnetic field structure in the vicinity of Earth's bow shock. Comparison is made between the laboratory measurements and earlier computer simulations in which ion gyromotion was included.

We wish to report what we believe to be the first observation in the laboratory of nonstationary collisionless shocks in magnetized plasma. Our experiments were conducted in a plasma wind tunnel designed to produce steady-state shock profiles. Details of this device and results of earlier measurements may be found elsewhere.<sup>1</sup> Recent refinements in our measurements, as described below, reveal that the interaction of an essentially steady plasma stream in the magnetosonic Mach-number range 4 to 8 with a fixed magnetic obstacle leads to a standoff shock which is not stationary. Rather, the plane containing the shock interface oscillates back and forth in the direction of the upstream plasma flow with a frequency comparable to the upstream ion gyrofrequency.

A large number of workers have reported observations of collisionless shocks in magnetized plasmas.<sup>2-5</sup> These observations were made on

radially imploding pinch devices, and to the best of our knowledge the fact that these shocks may be nonstationary has not been reported earlier. It may be argued that under conditions where the shock is produced by radial implosion, physical limitations in the available space preclude the observation of fluctuations within the shock interface on the time scale of the ion gyroperiod.

Recent observations<sup>6</sup> made by satellite-based sensors of Earth's bow shock may also be interpreted in terms of a nonstationary shock. Precursor compressions and rotations of the magnetic field on the upstream side of the shock, and fluctuations behind the shock of amplitude approximately 10 gammas are frequently observed. The origin of the precursor structure was concluded to be large-amplitude wave trains, which are frequently destroyed by changes in conditions at the shock. In light of our experiments, however, we feel that the possibility that

the bow shock undergoes rapid, irregular radial accelerations should not be ruled out. Such accelerations would also be consistent with the data for magnetic field versus time obtained from satellite observations on both the upstream and downstream sides of the bow shock.

We present our experimental observations next and conclude with a discussion which relates these observations to several theoretical arguments recently advanced to explain the mechanism of strong shock formation in collisionless, magnetized plasmas.

A plasma-wind-tunnel device is used to produce a standing shock wave, grossly stationary in the laboratory reference frame, for times long compared with an ion gyroperiod. This device is described in detail elsewhere.<sup>1</sup>

The shock wave is produced by the interaction of a supersonic plasma flow with the field of a magnetic obstacle. The obstacle is a set of straight, closely spaced, current-carrying conductors located on a diameter of the plasma-flow cross section, whose diameter is 70 cm at the half-density points. The upstream flow conditions are characterized by  $T_e = T_i$ ,  $\beta = 8\pi nk(T_e + T_i)/B^2 \cong 3$ , and Mach number  $M$  in the range 4 to 8. Here  $n$  is the particle density,  $k$  is Boltzmann's constant, and  $B$  is the magnetic field strength.

These conditions will be recognized as not untypical of the solar wind as it approaches the geomagnetic field. Directed ion energy in the upstream flow has been measured to be in excess of 100 eV, and consequently the mean free path for scattering of these primary ions by the ions of the shocked plasma is on the order of 1 m, much greater than the shock thickness. The neutral content of the flowing plasma has been measured, and found to be less than 5% of the ion density.

Figure 1 shows schematically the location of the obstacle conductors, the coordinate system, and the location of the shock wave. The flowing plasma approaches the obstacle from the left (negative  $x$ ), and a shock wave is observed to stand in the flow approximately 30 cm upstream from the obstacle, depending on the obstacle current and plasma flow energy. The components of the magnetic field just upstream and downstream of the shock are also shown in Fig. 1. On the upstream side,  $B_y$  and  $B_z$  are typically 15 to 20 G, while just behind the shock  $B_z$  is approximately 80 G and  $B_y$  has decreased to less than 5 G. While there is a field component  $B_x$

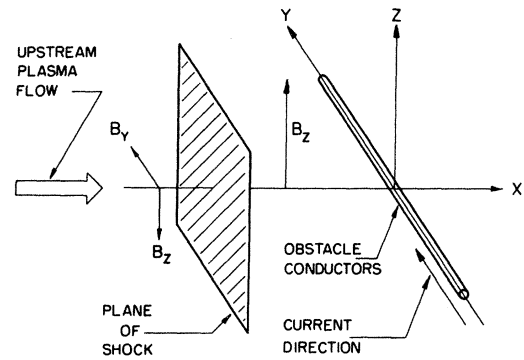


FIG. 1. Schematic diagram showing coordinate system, and relative positions of magnetic obstacle, shock wave, and upstream plasma flow.

of about 20 G far upstream, in the vicinity of the shock it has virtually vanished. The behavior of these fields is discussed more fully elsewhere.<sup>1</sup>

The presence of magnetic fluctuations in the shock region has previously been observed. Correlation of these fluctuations in space and time has now shown that the shock plane oscillates back and forth in the direction parallel to the upstream flow, at frequencies comparable to the upstream ion gyrofrequency ( $\sim 30$  kHz).

To correlate the magnetic fluctuations through the shock region in the  $x$  direction, a multiple magnetic probe is used. This probe has four coils oriented to sense  $B_z$  at 2-cm intervals along  $x$ . The integrated outputs from these coils are shown in Fig. 2(a). The slower-sweep (500  $\mu$ sec per division) photos show the behavior of  $B_z$  throughout the run, while the faster-sweep photos show the magnetic fluctuations during the central portion of the run. The observed correlation of the fluctuations leads to the conclusion that the shock wave, while grossly stationary in the lab frame, oscillates back and forth in an irregular fashion. In Fig. 2(b) we have plotted  $B_z$  vs  $x$  for two times  $t_1$  and  $t_2$ , indicated in Fig. 2(a) by arrows. Time-averaged values of  $B_z(x)$  are shown for positions outside the range of the multiple probe, with error bars indicating the amplitudes of the magnetic fluctuations at these points.

During the course of a run, the shock is observed to oscillate with an amplitude of 4 to 5 cm, compared to the previously measured<sup>1</sup> thickness of 6 to 8 cm. These dimensions are comparable with the "ion inertial length"  $c/\omega_{pi} = 8$  cm, but smaller than the ion gyroradius  $v_o/\Omega_i = 30$  cm. [ $c$  is the velocity of light,  $\omega_{pi}$  is the upstream ion plasma frequency,  $v_o$  is the up-

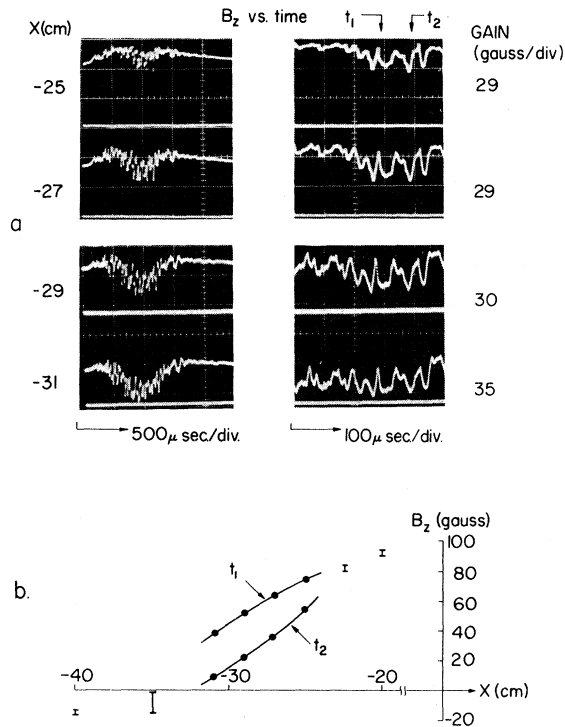


FIG. 2. (a) Integrated outputs from multiple probe coils sensing  $B_z$ . (b) Magnetic profile  $B_z(x)$  versus  $x$ . Curves labeled  $t_1$  and  $t_2$  drawn through points taken from (a) at times  $t_1$  and  $t_2$ . Error bars indicate range of  $B_z$  fluctuations at points outside range of multiple probe.

stream flow velocity, and  $\Omega_i$  is the ion gyrofrequency near the center of the shock ( $2\pi \times 75$  kHz).]

To determine that the magnetic oscillations are in phase in the  $z$  direction, magnetic probes sensing  $B_z$  were placed at 5-cm intervals above and below the system ( $x$ ) axis. The integrated outputs of these probes are shown in Fig. 3, and the oscillations are observed to be well correlated in the  $z$  direction. Similar experiments have shown good correlation in the  $y$  direction. The conclusion is that the magnetic structure of the shock oscillates in the  $x$  direction as a rigid body.

We have previously observed<sup>1</sup> that in order to change the time-average position of the shock wave by 4 cm, power supplied to the plasma accelerator must be changed by about 15%. When this is done, the magnetic field profile both upstream and downstream from the shock is considerably changed. In the experiments reported here, although the shock is oscillating with an amplitude of 4 cm, the upstream and downstream magnetic fields are quiet. Furthermore, no

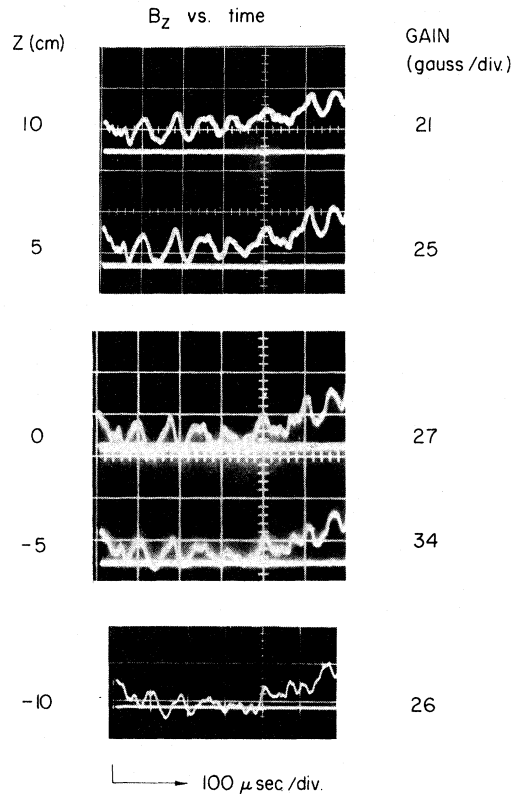


FIG. 3. Integrated outputs from magnetic probes sensing  $B_z$  at positions  $x = -32$  cm,  $y = 0$ , and  $z$  as noted.

sign of the  $\Omega_i$  activity is observed by the current and voltage monitors on the plasma accelerator. We therefore conclude that the oscillations are an inherent part of the shock structure, rather than due to power fluctuations from the accelerator.

It is generally believed that weak shocks,  $M_A \lesssim 3$  ( $M_A$  being the Alfvén Mach number), may be understood in terms of fluid theories which take into account anomalous resistivity induced by electron streaming in the plane of the shock, where the streaming arises from magnetic gradients. Although many details remain to be resolved, there is generally good agreement between experimental observation and theoretical predictions for this regime.

Strong shocks, where resistive dissipation is not sufficient to produce relaxation, require an anomalous "ion viscosity" for shock formation. This is consistent with the observation that in strong shocks the ions are more strongly heated than the electrons. It has been suggested<sup>7,8</sup> that ion counterstreaming instabilities can lead to

levels of plasma turbulence sufficient to produce anomalous "ion viscosity." A careful examination of this problem<sup>9</sup> reveals that this instability mechanism is operative only as long as  $T_i/T_e$  is sufficiently low. For  $T_i/T_e \gtrsim 0.6$  the growth rates decrease to values comparable to ion gyrofrequencies, and it becomes essential to take into account ion gyromotion. Similar reservations may be expressed with regard to the electron cyclotron drift instability proposed by Forslund, Morse, and Nielson.<sup>10</sup>

Recent macroparticle computer calculations on electrostatic shocks<sup>11</sup> have shown some success in producing stationary shocks over a limited range of  $T_i/T_e$  and Mach number. Extension of this approach to magnetosonic shocks, in which the electrons are treated as magnetized but the Lorentz force on the ions is neglected, leads to results rather similar to the electrostatic ( $B=0$ ) ones.<sup>12</sup> More recently it has been reported<sup>13</sup> that such a model in which ion gyromotion is neglected leads to stationary shock formation for  $M_A > 3$ .

The experimental results presented here appear to lend credence to the earlier computer-simulation studies which included ion gyromotion.<sup>14-16</sup> In these computations one observes only quasi-stationary shocks with significant fluctuation on the ion gyrofrequency scale and higher within the shock structure. On the evidence of these calculations it has been argued<sup>9,17</sup> that ion gyromotion induces large-scale fluctuations and a resultant coarse graining in the ion velocity distribution at high Mach numbers. Fine-scale instabilities may then help smooth the distribution towards a final equilibrium state.

We plan to continue these experiments with

principal attention being focused on understanding the details of shock formation, energy partition, and thermal relaxation under the high-Mach-number conditions approximating Earth's bow shock.

\*Work supported by the National Science Foundation under Grant No. GA-31175

<sup>1</sup>D. L. Morse and W. W. Destler, to be published.

<sup>2</sup>J. W. M. Paul, G. C. Goldenbaum, A. Iiohshi, L. S. Holmes, and R. A. Hardcastle, *Nature* **216**, 363 (1967).

<sup>3</sup>M. Keilhacker, M. Kornherr, and K.-H. Steuer, *Z. Phys.* **223**, 385 (1969).

<sup>4</sup>R. Kh. Kurtmullaev, V. L. Masolov, K. I. Mekler, and V. I. Pil'skii, *Zh. Eksp. Teor. Fiz., Pis'ma Red.* **7**, 65 (1968) [*JETP Lett.* **7**, 49 (1968)].

<sup>5</sup>M. Martone and S. E. Segre, *Plasma Phys.* **12**, 205 (1970).

<sup>6</sup>R. W. Fredricks, G. M. Crook, C. F. Kennel, I. M. Green, F. L. Scarf, P. J. Coleman, and C. T. Russell, *J. Geophys. Res.* **75**, 3751 (1970).

<sup>7</sup>D. A. Tidman, *J. Geophys. Res.* **72**, 1799 (1967).

<sup>8</sup>B. Bertotti and D. Biskamp, European Space Research Organization, Special Paper No. SP-51, 41, 1969 (unpublished).

<sup>9</sup>P. L. Auer, R. W. Kilb, and W. F. Crevier, *J. Geophys. Res.* **76**, 2927 (1971).

<sup>10</sup>D. W. Forslund, R. L. Morse, and C. W. Nielson, *Phys. Rev. Lett.* **25**, 1266 (1970).

<sup>11</sup>D. W. Forslund and C. R. Shonk, *Phys. Rev. Lett.* **25**, 1266 (1970).

<sup>12</sup>R. J. Mason, private communication.

<sup>13</sup>K. Papadopoulos, C. E. Wagner, and I. Haber, *Phys. Rev. Lett.* **27**, 982 (1971).

<sup>14</sup>P. L. Auer, H. Hurwitz, Jr., and R. W. Kilb, *Phys. Fluids* **5**, 298 (1962).

<sup>15</sup>V. J. Rossow, *Phys. Fluids* **8**, 358 (1965).

<sup>16</sup>V. J. Rossow, *Phys. Fluids* **10**, 1056 (1967).

<sup>17</sup>P. L. Auer and W. H. Evers, Jr., *Phys. Fluids* **14**, 1177 (1971).

## Onset of Ballistic Temperature Pulses in Solid $^4\text{He}$ ‡

J. N. Fox,\* J. U. Trefny, J. Buchanan,§ L. Shen, and B. Bertman†  
*Department of Physics, Wesleyan University, Middletown, Connecticut 06457*  
 (Received 1 November 1971)

We observe the onset of the ballistic flow of phonons using temperature pulse techniques below 0.2 K in solid  $^4\text{He}$  crystals grown from the superfluid. First-sound velocities obtained from these measurements compare satisfactorily with ultrasonic measurements recently reported.

At the present time there is considerable interest in the propagation of temperature pulses in dielectric solids.<sup>1</sup> Depending upon the dominant phonon scattering mechanism, temperature pulses may propagate ballistically, travel as second

sound, or decay by diffusion. Second-sound pulses and diffusive behavior have been previously observed in crystals of  $^4\text{He}$ .<sup>2</sup> In this Letter we report the detection of ballistic flow in solid  $^4\text{He}$ , and compare the pulse arrival times with recent

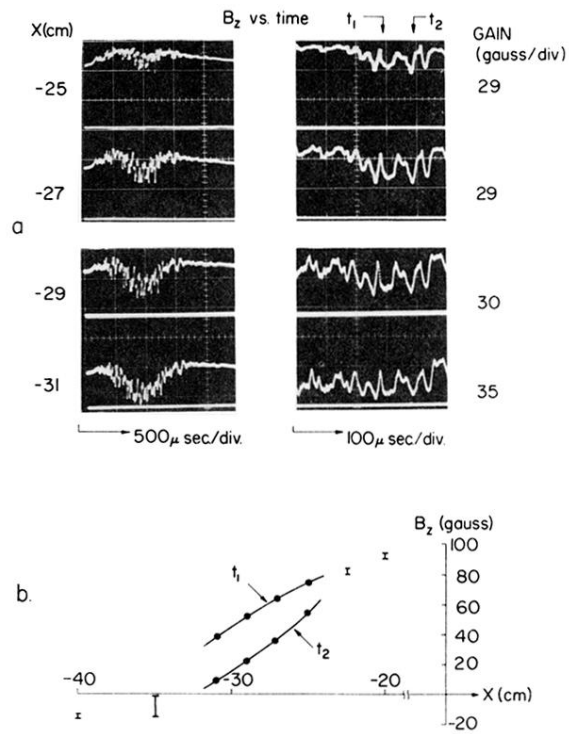


FIG. 2. (a) Integrated outputs from multiple probe coils sensing  $B_z$ . (b) Magnetic profile  $B_z(x)$  versus  $x$ . Curves labeled  $t_1$  and  $t_2$  drawn through points taken from (a) at times  $t_1$  and  $t_2$ . Error bars indicate range of  $B_z$  fluctuations at points outside range of multiple probe.

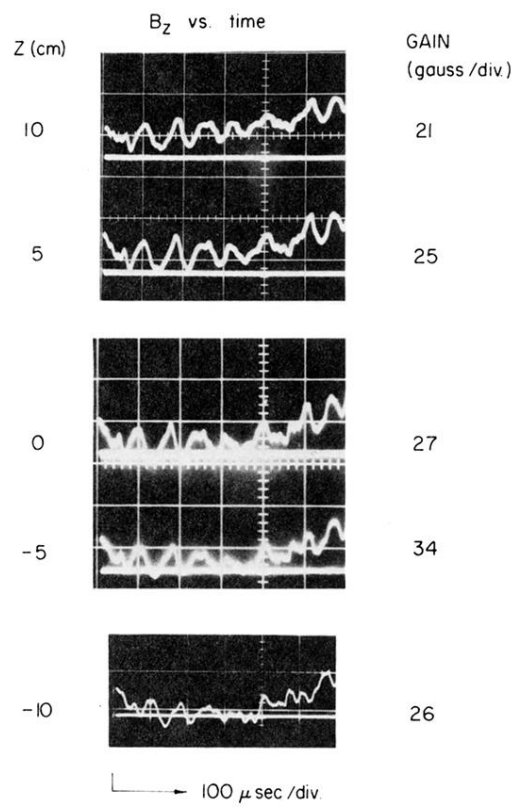


FIG. 3. Integrated outputs from magnetic probes sensing  $B_z$  at positions  $x = -32$  cm,  $y = 0$ , and  $z$  as noted.